ISSN 1063-7834, Physics of the Solid State, 2007, Vol. 49, No. 11, pp. 2080–2085. © Pleiades Publishing, Ltd., 2006.
Original Russian Text © S.S. Aplesnin, L.I. Ryabinkina, O.B. Romanova, D.A. Balaev, O.F. Demidenko, K.I. Yanushkevich, N.S. Miroshnichenko, 2007, published in Fizika Tverdogo Tela, 2007, Vol. 49, No. 11, pp. 1984–1989.

SEMICONDUCTORS AND DIELECTRICS

# Effect of the Orbital Ordering on the Transport and Magnetic Properties of MnSe and MnTe

**S. S. Aplesnin[a, b], L. I. Ryabinkina[a], O. B. Romanova[a], D. A. Balaev[a], O. F. Demidenko[c], K. I. Yanushkevich[c], and N. S. Miroshnichenko[b]**

[a] *Kirensky Institute of Physics, Siberian Branch, Russian Academy of Sciences, Krasnoyarsk, 660036 Russia*
*e-mail: rob@iph.krasn.ru*

[b] *Reshetnev Siberian State Aerospace University, Krasnoyarsk, 660014 Russia*

[c] *Joint Institute of Solid State and Semiconductor Physics, National Academy of Sciences of Belarus, Minsk, 220072 Belarus*

Received February 26, 2007; in final form, April 27, 2007

**Abstract**—This paper reports on the results of measurements of the conductivity in MnSe and MnTe polycrystalline samples under thermal cycling in the temperature range $80 < T < 300$ K in magnetic fields of up to 5 kOe. Manganese selenide MnSe is found to exhibit a magnetoresistive behavior below the Néel temperature. The specific features revealed in the temperature dependences of the magnetic susceptibility and the electrical resistivity in some temperature ranges are accounted for in terms of magnetic ordering, which is mediated by the interaction of the pseudoorbital moments with spins.

PACS numbers: 71.35.–y, 71.45.Gm

**DOI:** 10.1134/S106378340711011X

## 1. INTRODUCTION

Manganese chalcogenides MnS, MnSe, and MnTe undergo structural and magnetic transitions with an increase in the extent of manganese ion hybridization with the S, Se, and Te anions. The transport properties of these compounds can change from semiconducting to metallic. The ZnSe/MnSe-based multilayers are currently used in magnetooptical devices [1]. Multilayer GdTe/MnTe films [2] are attracting intense interest for possible applications in the field of information recording. These compositions conduct current by the polaron mechanism which is sensitive to even extremely small changes in unit cells of the magnetic and crystal structures. Manganese chalcogenides are antiferromagnets (AF). The MnS sulfide crystallizes in a NaCl-type structure, and MnTe, a NiAs-type hexagonal [3]. Manganese monoselenide MnSe undergoes a structural phase transition from the cubic to NiAs structure in the temperature range $248 < T < 266$ K [3], and below this temperature two phases are observed to coexist, the NiAs phase amounting up to 30%, and the cubic phase occupying the remaining 70% of the sample volume [4]. The magnetic phase transition temperature, as derived from neutron diffraction studies [5], is $T_N = 135$ K for MnSe in the cubic modification, while in the hexagonal NiAs phase it coincides with the structural transition point $T_s = 272$ K. Manganese chalcogenides are *p*-type semiconductors with an energy gap in the single-particle electron excitation spectrum for MnS (2.7–2.8 eV), MnSe (2.0–2.5 eV), and MnTe (0.9–1.3 eV) [6]. The changes in the temperature dependence of the electrical resistivity in MnSe and MnTe near the Néel temperature were attributed in [7] to the interaction of charge carriers with localized spins.

We focus our attention here on some effects observed in the MnSe and MnTe semiconductors that still have not found proper explanation. To begin with, MnSe exhibits a strong maximum in magnetic susceptibility in the temperature range $T = 160$–$180$ K, i.e., above the Néel temperature for the cubic modification. At $T \sim 200$ K, the temperature dependence of the MnSe magnetic susceptibility passes through a minimum, which cannot be assigned to superposition of susceptibilities for the AF MnSe having a cubic and a nickel–arsenide structure. The hyperfine magnetic field generated by the orbital, spin, and multipole $(LS)L + L(LS)$ moments has a minimum at $T \sim 180$ K, and the temperature dependences of the quadrupole interaction parameters, such as the derivatives of the axial and longitudinal electric field components, exhibit a maximum close to these temperatures [8]. One observes also a slight decrease in the lattice parameters within a few thousandths of an angstrems [9] for $T < 180$ K. The temperature dependence of the lattice thermal expansion coefficient was found to pass through a strong maximum as high as $\alpha = 10^{-4}$ K$^{-1}$ at $T = 190$ K [10]. Some nuclear peaks measured in neutron diffraction below the point of magnetic phase transformation ($T < 260$ K) were observed to broaden [11]. Similar phenomena were found to exist in manganese monotelluride as well. The

intensities of the (002) nuclear reflection seen in the neutron diffraction patterns of MnTe are smaller than those calculated for the NiAs hexagonal structure [10] and vary very little for $T < 100$ K [9]. One observes an increase in the lattice parameter ratio from $c/a = 1.607$ at $T = 90$ K to $c/a = 1.615$ at $T = 75$ K [9]. Attenuation of the nuclear acoustic resonance caused by the spins of nuclei and electrons exhibits additional, frequency-independent absorption at $T \sim 90$ K [12, 13]. The magnetization and the electrical resistivity of polycrystalline MnTe samples behave anomalously with temperature in the vicinity of $T \sim 90$ K [9]. Manganese telluride reveals a crossover from the semiconducting to metallic behavior. One observed a noticeable growth of magnetic susceptibility resembling that accompanying the transition to the ferromagnetic (FM) state. Neutron diffraction studies performed in the temperature region from 10 to 300 K did not substantiate the existence of additional superstructural reflections in the diffraction patterns of either MnTe or MnSe [4, 5]. It is these observations that have motivated our study as a search for a possible additional mechanism that could influence the transport and magnetic properties of the transition metal chalcogenides MnSe and MnTe.

## 2. SAMPLE PREPARATION AND EXPERIMENTAL RESULTS

The MnSe and MnTe samples were prepared in evacuated quartz ampoules heated in resistance furnaces in a stepped regime. The charge consisted of a mixture of powdered selenium, tellurium, and manganese. The selenium and tellurium were of 99.99% purity, and manganese was not worse than 99.8% pure. The components of the charge were placed in precisely calculated amounts into the quartz ampoules with special precautions to maintain the stoichiometry of the composition, evacuated, and mixed thoroughly. During the first day, the temperature did not exceed 720 K, and during the next three days it was maintained at about 920 K. Subsequently, the temperature was raised to 1370 K for two hours, followed by quenching of the ampoules in cold water. The products obtained in the first sintering were crushed and pressed into cylindrical rods for subsequent homogenization anneal. The annealing was performed in evacuated quartz ampoules during four days at $T = 1120$ K. On the fifth day, the temperature was raised to 1370 K for two hours, after which the ampoules with the samples were likewise quenched in cold water.

The electrical resistivity of the synthesized MnSe and MnTe samples was measured by the four-probe technique. Heating and cooling of the MnSe sample revealed hysteresis in the region of $125 < T < 260$ K, the temperatures corresponding to the coexistence of the cubic and hexagonal modifications. Incidentally, for MnSe the resistance hysteresis loop traces a figure-eight profile, which depends on the rate of temperature variation during the experiment. The $R(T)$ curves

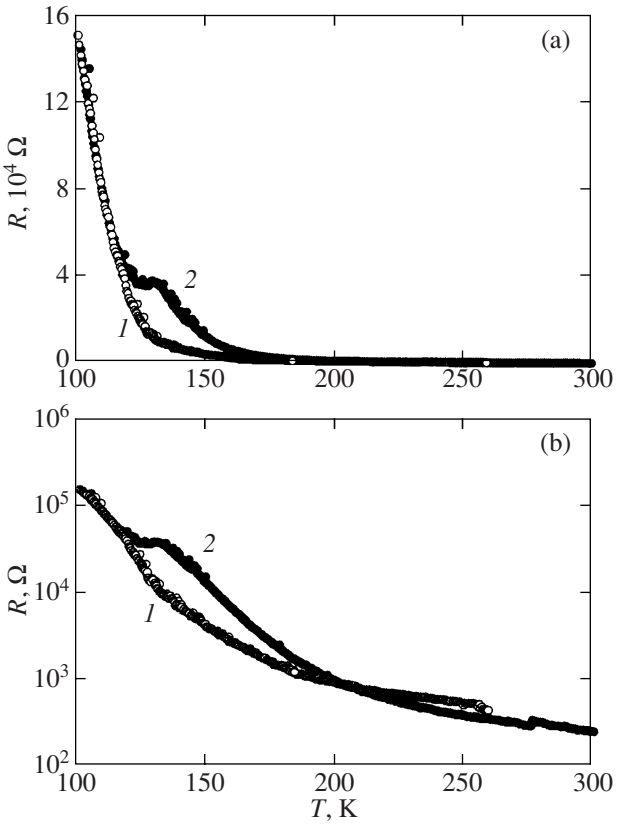


**Fig. 1.** Temperature dependences of the electrical resistivity of MnSe with the temperature changed in 1 h by (a) 10 and (b) 30 K: (*1*) heating and (*2*) cooling.

obtained in the heating and cooling modes are observed to cross at $T \sim 200$ K (Fig. 1). Thermal cycling in the temperature region $200 < T < 300$ K does not reveal any resistance hysteresis.

The temperature dependence of the electrical resistivity of MnTe provides evidence for a transition from the metallic to semiconducting state. The $\rho(T)/\rho(295\ \text{K}) = f(T)$ graph reveals a maximum in the electrical resistivity near $T_N = 320$ K and a sharp change in the resistivity by an order of magnitude (Fig. 2). In the low-temperature region, our results are in agreement with the data reported in [9]. The overall pattern of the dependence $\rho(T)$ for MnTe resembles closely that of the electrical resistivity on the temperature for manganites, for instance, for $La_{0.275}Pr_{0.35}Ca_{0.375}MnO_3$ [14], where at $T_c = 150$ K one observed a metal–insulator transition, and the increase in the resistivity below $T = 210$ K was assigned to the formation of a phase with a disordered charge distribution.

The MnSe samples exhibited magnetoresistance in the magnetically ordered cubic phase. The magnetoresistance increases as one approaches the Néel temperature. Indeed, at $T = 100$ K the magnetoresistance measured at $H = 5$ kOe is $\delta_H = (\rho(H) - \rho(0))/\rho(H) = -4.8\%$,

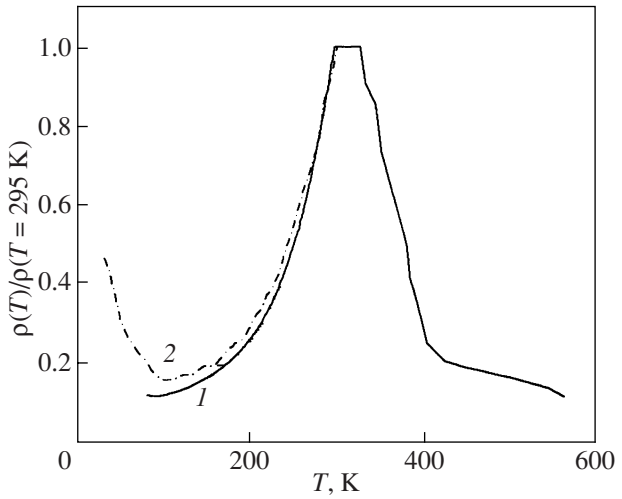


**Fig. 2.** Temperature dependences of the electrical resistivity normalized to ρ at $T = 295$ K for MnTe: (*1*) our date and (*2*) data taken from [9].

while at $T = 113$ K $\delta_H = -14\%$. The behavior of resistance with external magnetic field is plotted in Fig. 3.

## 3. DISCUSSION OF THE RESULTS

We attempt to interpret our experimental results by assuming that the main charge carrier is the charged exciton formed in *d–p* hybridization of manganese cations with the anions of selenium and tellurium. The semiconductors under study have mixed, ionic and covalent bonding. It is known that the charge gap associated with charge transfer from an anion to a cation decreases as the anion crosses over from S to Te. The gap is $\Delta = \varepsilon_d - \varepsilon_p = 1.5, 0.8, 0$ eV for MnS, MnSe, and MnTe, accordingly. The *p–d* hybridization energy, which is proportional to $r^{-3.5}$ [16], decreases too: $V_{pd} = -1.2, -1.0, -0.8$ eV [15]. The distance $r$ between the cations of manganese and anions increases in the series MnS (2.61 Å), MnSe (2.73 Å), MnTe (2.92 Å). If the single-particle electronic excitation spectrum in the above compounds has a gap, fluctuations in orbital excitations will also open a gap in the spectrum of two-particle excitations, which are generated by transfer of electronic density distribution on the cation–anion bond over the lattice, as a result of interaction with phonon excitations of the lattice. The longitudinal and transverse modes of optical vibrations are localized in the frequency range $\omega = 190$–$220$ cm$^{-1}$ [17]. The Raman spectrum of the $Mn_xGd_{1-x}Te$ solid solutions [18] reveals a frequency shift representing a combination of optical phonon and magnon frequencies. This can be considered as evidence for the Fröhlich mechanism of electron–phonon coupling. Electron–phonon coupling gives rise to formation of lattice polarons which become pinned to lattice defects and at polycrystal boundaries to create local static lattice distortions.

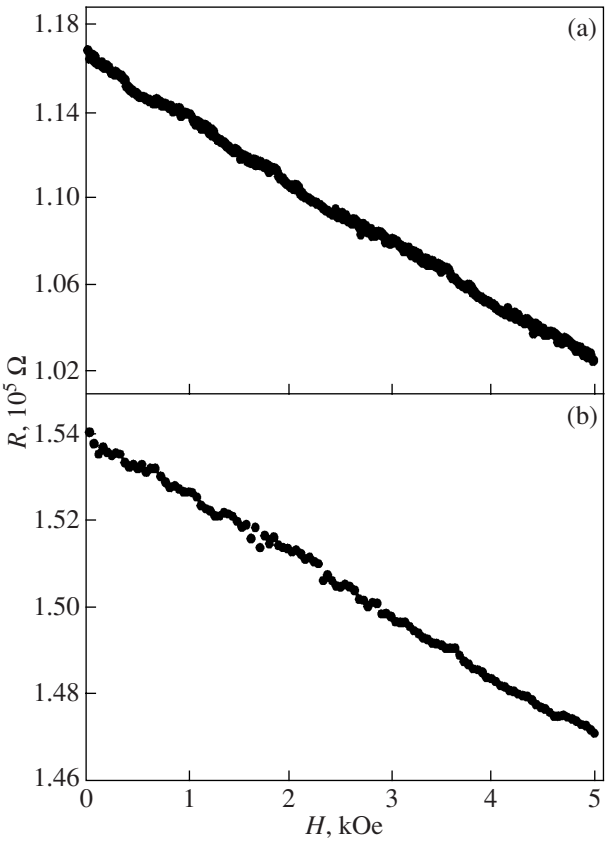


**Fig. 3.** Dependences of the resistance of MnSe on the external magnetic field for temperatures $T$ = (a) 113 and (b) 100 K.

For MnSe, the pinning of lattice polarons at $T_1 = 175$ K can probably be attributed to the torsional mode. The $d_{z^2}$–$p_z$–$d_{z^2}$ orbitals are not involved in charge transfer among neighboring sites because the phases of the $d_{z^2}$ orbitals coincide. One can therefore conceive here of two scenarios of charge transfer from one site to another, $d_{z^2j}$–$p_{zi}$–$p_{xi}$–$d_{z^2k}$ and $d_{z^2j}$–$p_{zi}$–$p_{yi}$–$d_{z^2k}$, i.e., the charge on an anion can transfer from the $p_z$ orbital to either $p_x$ or $p_y$. These transitions are degenerate, and the degeneracy is lifted by interaction with elastic vibrational modes at a temperature $T_1$. This changes the exchange interaction energy because of competition between the mechanisms mediated by conduction electrons and indirect exchange involving the $t_{2g}$ orbitals. These changes in the exchange and hopping integral parameters are governed by the magnitude of electron–phonon interaction and should become manifest in some characteristic wave vector.

To form a qualitative idea of the above effects, assume that the charge density at hybridized orbitals changes below some temperature. This can be presented mathematically via orbital ordering of orbital

pseudospins and spin ordering described by the Hamiltonian

$$H = -\sum_{ij} J_{ij} S_i S_j - \sum_{ij} A_{ij} \tau_i \tau_j - 4 \sum K_{ijlm} S_i S_j \tau_l \tau_m,$$

where $J_{ij}$ is the exchange interaction, which is negative along the hexagonal axis ($J < 0$) and positive ($J > 0$) in the hexagonal plane; the orbital interaction parameter $A_{ij} \sim g^2/\omega_k$ ($g$ is the electron–phonon coupling constant, and $\omega_k$ is the phonon optical frequency); and $K$ is the coupling parameter of the orbital with the spin subsystems, which depends on the interband hopping integrals $t_{\alpha\beta}$ ($\alpha, \beta = p_x, p_y, p_z$) and gap width $\Delta$ in the electronic excitation spectrum: $K = t_{\alpha\beta}^2/\Delta$. The Hamiltonian derived from the many-electron Hamiltonian [19] is strongly anisotropic in pseudospins, but this anisotropy can be neglected in a qualitative analysis of a structure.

As can be seen from the optical spectra [18] with a minimum in the longitudinal optical vibration branch at the zone center, $\omega_{k=0} = \omega_0$, in MnTe interaction between hybridized orbitals, $d_{z^2 j}$–$p_{zi}$–$p_{xi}$–$d_{z^2 k}$, is mediated by longitudinal optical phonons. The orbital ordering parameter passes through a maximum at $k = 0$, i.e., the orbitals are FM ordered. In MnSe, interaction between orbitals is mediated by the torsional mode, with the maximum of interaction at a wave vector $Q$. This assumption is qualitatively substantiated by the broadening of nuclear Bragg reflections below $T <$ 260 K, which sometimes is treated as due to a stacking fault of the hexagonal lattice at a length equal to three lattice constants [10]. The model we are proposing assumes alternation of the $p_x$ and $p_y$ hybridized orbitals with a certain period. The spins are in-plane ferromagnetically ordered, and neighboring planes are directed oppositely to one another. This results in an ordering competition between the spin and orbital subsystems.

The clearly pronounced changes in the quadrupole interaction parameters, lattice parameters, and linear expansion coefficients strongly suggest that the orbital ordering temperature in MnSe is $T_{\text{orb}} \approx 180$ K. A characteristic feature of the compounds under study is the change in the type of short-range order for $T > T_{\text{orb}}$ caused by the competing interactions. One can assume the existence in the temperature region $T_{\text{orb}} < T < T_{\text{N}}$ of a structure incommensurate in orbital ordering, which is induced by the spin subsystem. In MnTe, the changes observed to occur in nuclear reflection intensity and lattice parameters below $T = 90$ K give grounds to associate this temperature with FM ordering of orbitals. The orbital ordering gives rise to a growth of orbital correlation functions $\langle \tau_q \tau_{-q} \rangle$ and renormalization of the exchange interaction parameters. Indeed, the Hamiltonian suggests that $J_{ij}^{\text{eff}} = J_{ij} + 4K_{ijlm}\langle \tau_l \tau_m \rangle$. In MnTe, the correlator is proportional to magnetization $\langle \tau_l \tau_m \rangle = \langle \tau \rangle^2$, the temperature dependence of squared magnetization considered in molecular field approximation is linear, $A(1 - T/T_{\text{orb}})$. The exchange interaction modulus decreases with decreasing temperature, $J^{\text{eff}} = J(1 - 4\lambda(1 - T/T_{\text{orb}}))$, where $\lambda \sim K/J$. The AF susceptibility for polycrystalline samples can be written as $\chi = 1/3\chi^{zz} + 2/3\chi^{x,y}$. The susceptibility over transverse components in a magnetically ordered region, considered in the molecular field approximation, does not depend on temperature, and that over the longitudinal spin components grows nonlinearly from zero to a finite value $\chi(T_{\text{N}}) = C/(2T_{\text{N}})$. Because we are considering effects here on the qualitative level, the temperature dependence of susceptibility can be approximated by a quadratic function of temperature $\chi(T) = (C/6)(2 + T/T_{\text{N}})^2/J^{\text{eff}}$ for $T < T_{\text{N}}$ and $\chi(T) = C/(T_{\text{N}}(1 + T/T_{\text{N}}))$ for $T > T_{\text{N}}$.

Figure 4a displays the normalized temperature dependences of the susceptibility of MnTe for different parameters of interaction of the orbital with spin subsystems. A comparison with experimental data on the susceptibility [9] yields about 18% for the parameter of interaction between the orbital and spin subsystems. In MnSe, long-range order with the structure vector $Q$ sets in below the orbital ordering temperature. The pseudospin correlator

$$\langle \tau_Q \tau_{-Q} \rangle = \frac{1}{N} \sum_q \tau_q \tau_{-q} = T\chi_{\text{orb}}(T)$$

can be expressed in terms of the orbital susceptibility, whose temperature dependence conforms qualitatively to that of the AF susceptibility. The renormalized exchange parameter in MnSe can be written as $J_{ij}^{\text{eff}} = J(1 - 4\lambda T\chi_{\text{orb}}(T)/J)$; it takes on the lowest value at $T = T_{\text{orb}}$, thus bringing about a maximum in the magnetic susceptibility. Figure 4b plots the susceptibility of MnSe calculated with inclusion of the variations in exchange parameters. The susceptibility of MnSe includes a contribution of the cubic modification reaching a maximum near the Néel temperature, which makes estimation of the interaction parameter for the orbital and spin subsystems a hard problem. It does not, however, exceed $K/J \approx 0.1$, which follows from a comparison of the normalized susceptibility maxima at the Néel temperature and the temperature of orbital ordering $T_{\text{orb}}$.

Neutron diffraction studies of the magnetic and crystal structures of MnSe performed in [5] furnish direct evidence for the existence of orbital ordering. Indeed, the temperature dependence of the total intensity of the (1/2,1/2,1/2) and (001) reflections plotted in Fig. 4c has three breaks, namely, the first of them in the range 135–138 K, the second in the range of 180–190 K, and the third, at 250–275 K. The first and the third breaks were attributed [5] to the transition from

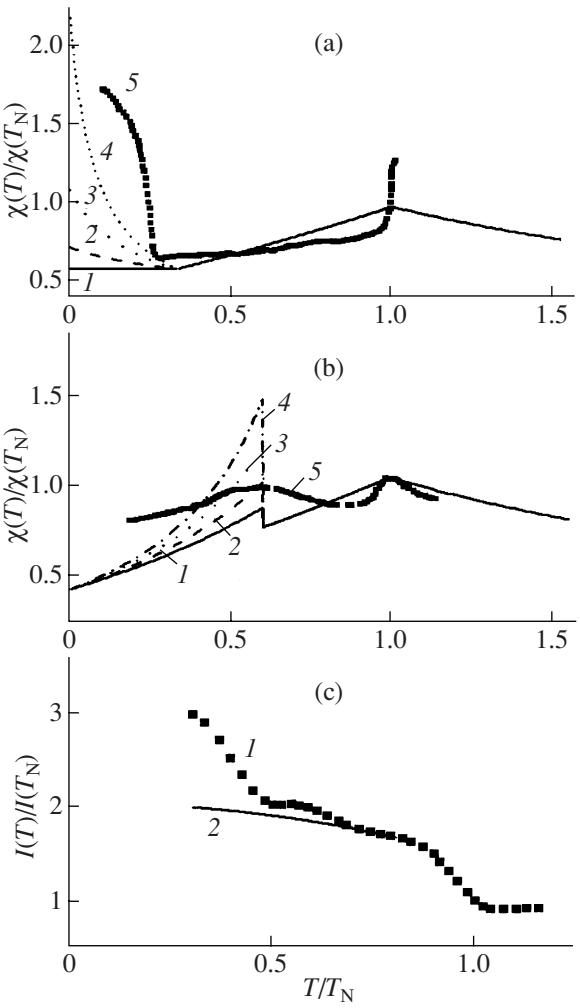


**Fig. 4.** Susceptibility calculated in the molecular field approximation for different parameters of coupling between the orbital and spin subsystems as a function of the temperature normalized to the Néel temperature. $K/J$ = (*1*) 0.05, (*2*) 0.10, (*3*) 0.15, and (*4*) 0.20. (*5*) Experimental dependences $\chi(T)/\chi(T_N)$ for (a) MnTe [9] and (b) MnSe [4]. (c) (*1*) Normalized intensity of (1/2,1/2,1/2) and (001) reflections in MnSe as a function of the normalized temperature $T/T_N$ [5] and (*2*) the interpolation of the normalized intensity $I(T)/I(T_N) = 2.05 - 0.57(T/T_N)^2$.

the cubic to hexagonal MnSe modification, respectively, i.e., from the antiferromagnetic to paramagnetic state. The temperature corresponding to the break in the temperature dependence of the intensity at 181 K fits well the calculated temperature of orbital ordering. Low-temperature approximation of the intensity, $I(T) = S^2(q)$ ($S(q)$ is the magnetic structural factor), for the AF state assumes the form $I(T)/I(T_N) = 2.05 - 0.57(T/T_N)^2$ (solid line in Fig. 4c). The difference in the intensities shown by the upper and lower curves in Fig. 4c at $T/T_N = 0.5$ permits estimation of the structural orbital factor $S_L^2(Q) \sim (I_{up} - I_{down} - 1)$. We come to $(I_{up} - I_{down} - 1)/(I_{down} - 1) \approx 0.1$. Knowing the spin structural factor $S^2(q) \approx 20$ [6], we obtain $S_L^2(Q) \approx 2$ and arrive at the effective magnetic orbital moment of about ~1.4. This value of the orbital moment can probably be assigned to the existence of short-range spin order in the transition from the antiferromagnetic to paramagnetic state in the cubic phase.

At temperatures $T_{orb} < T < T_N$, there exist regions with short-range order corresponding to ordering of some type of orbitals; regions with another type of orbitals can, however, also appear, which should lead to formation of a charge-disordered state similar to the one observed in manganites [14]. The electrostatic and exchange interaction of carriers with the elastic and magnetic subsystems will bring about formation of quasi-degenerate states and spin glass effects. Indeed, Coulomb interaction inducing lattice structure distortions competes with exchange interactions, which change the electron kinetic energy and the exchange field. Orbital (charge) ordering entails a decrease in the magnetic moment on a site, and in the limiting cases of strong interaction between the spin and orbital subsystems ($K \gg J, A$) it will lead to disappearance of long-range order and formation of the spin liquid state. This model accounts for the decrease in the magnetic moment in MnSe down to $\mu = 4.45\mu_B$, and in MnTe, to $\mu = 4.7\mu_B$ [6].

## 4. CONCLUSIONS

The interpretation of the above experimental data permits the following conclusion: the interaction of hybridized anion orbitals with lattice phonons is capable of initiating orbital ordering at a critical temperature. This will entail a change in the effective exchange interaction parameter and the magnetic susceptibility. Competition between the exchange and orbital interactions induces incommensurate orbital ordering in the temperature range $T_{orb} < T < T_N$ and can give rise to spin glass effects, which become manifest in specific features in the behavior of the temperature dependences of the electrical resistivity.

## ACKNOWLEDGMENTS

This study was supported by the Russian Basic Research Foundation (project RFFI–BRFFI no. 04-02-81018 Bel 2004a)

## REFERENCES

1. I. P. Smorchkova, N. Samarth, J. M. Kikkawa, and D. D. Awschalom, Phys. Rev. Lett. **78**, 3571 (1997).
2. S. Scholl, J. Gerschutz, F. Fischer, A. Waag, D. Hommel, K. Von Schierstedt, B. Kuhn-Heintich, and G. Landwehr, Appl. Phys. Lett. **62**, 3010 (1993).
3. D. L. Decker and R. L. Wild, Phys. Rev. B: Solid State **4**, 3425 (1971).

4. J. B. C. Efrem, D. Sa, P. A. Bhobe, K. R. Priolkar, A. Das, P. S. Krishna, P. R. Sarode, and R. B. Prabhu, J. Phys. **63**, 227 (2004).
5. G. I. Makovetskii and A. I. Galyas, Fiz. Tverd. Tela (Leningrad) **24** (9), 2753 (1982) [Sov. Phys. Solid State **24** (9), 1558 (1982)].
6. S. J. Youn, B. I. Min, and A. J. Freeman, Phys. Status Solidi B **241**, 1411 (2004).
7. P. G. De Gennes and J. Friedel, J. Phys. Chem. Solids **4**, 71 (1958).
8. R. J. Pollard, V. H. McCann, and J. B. Ward, J. Phys. C: Solidi State Phys. **16**, 345 (1983).
9. J. B. C. Efrem, D. Sa, P. A. Bhobe, K. R. Priolkar, A. Das, S. K. Paranjpe, R. B. Prabhu, and P. R. Sarode, cond-mat/0408124.
10. T. Ito, K. Ito, and M. Oka, Jpn. J. App. Phys. **17**, 371 (1978).
11. A. J. Jacobson and B. E. F. Fender, J. Phys. Chem. **52**, 4563 (1970).
12. N. Kunitomi and Y. Hamaguchi, J. Phys. (Paris) **25**, 568 (1964).
13. K. Walther, Phys. Rev. B: Solid State **4**, 3873 (1971).
14. N. D. Mathur, G. Burnell, S. P. Isaac, T. J. Jackson, B.-S. Teo, J. L. MacManus-Drtiscoll, L. F. Cohen, J. E. Evetts, and M. G. Blamier, Nature (London) **387**, 266 (1997).
15. H. Sato, T. Mihara, A. Furuta, M. Tamura, K. Mimura, N. Happo, M. Taniguchi, and Y. Ueda, Phys. Rev. B: Condens. Matter **56**, 1722 (1997).
16. W. A. Harrison, *Electronic Structure and the Properties of Solids* (Freeman, San Francisco, 1980).
17. A. K. Arora, E. K. Suh, U. Debska, and A. K. Ramdas, Phys. Rev. B: Condens. Matter **37**, 21927 (1988).
18. A. Milutinovic, N. Tomic, S. Devic, P. Milutinovic, and Z. V. Popovic, Phys. Rev. B: Condens. Matter **66**, 012302 (2002).
19. K. I. Kugel' and D. I. Khomskiĭ, Usp. Fiz. Nauk **136** (4), 621 (1982) [Sov. Phys. Usp. **25** (4), 231 (1982)].

*Translated by G. Skrebtsov*